

## Electrochemical Growth of a $\text{Cu}_2\text{O}/\text{PbS}$ Epitaxial Heterojunction on Single Crystal Au(100)

Alexey A. Vertegel, Mark G. Shumsky, and Jay A. Switzer\*

University of Missouri–Rolla, Department of Chemistry and Graduate Center for Materials Research, Rolla, Missouri 65409-1170

Received November 4, 1999

Revised Manuscript Received February 1, 2000

Semiconductor heterojunctions are ideal for light-harvesting devices such as photovoltaic<sup>1,2</sup> and photoelectrochemical<sup>3</sup> cells, since multiple-semiconductor devices can absorb a larger fraction of the solar spectrum than single-semiconductor devices. Epitaxial heterojunctions are desired for these applications since the transport of photogenerated electrons or holes across the interface is more efficient. In addition, multilayered semiconductor heterojunctions show quantum confinement effects in the small band-gap semiconductor when the layer thicknesses are in the nanometer range.<sup>4</sup> It is often possible to electrodeposit multilayered architectures from a single plating bath by simply pulsing the applied potential during growth.<sup>5–11</sup> The low processing temperatures (often room temperature) of electrodeposition should lead to abrupt interfaces in epitaxial heterojunctions, because interdiffusion will be minimized.

Lincot and co-workers have used electrodeposition to prepare epitaxial films of CdTe on InP<sup>12</sup> and ZnO on GaN.<sup>13</sup> Our emphasis has been on the electrodeposition of epitaxial structures with a large lattice mismatch. We have recently shown that epitaxial films of individual semiconductors such as  $\text{Bi}_2\text{O}_3$ ,<sup>14</sup>  $\text{Cu}_2\text{O}$ ,<sup>15</sup> and  $\text{PbS}$ <sup>16</sup> can be electrodeposited onto single-crystal Au.

\* To whom correspondence should be addressed. E-mail: jswitzer@umr.edu.

(1) Sze, S. E. *Physics of Semiconductor Devices*, 2nd ed.; Wiley: New York, 1981; Chapter 14.

(2) Bolton, J. R.; et al. *Nature* **1985**, *316*, 495.

(3) Khaselev, O.; Turner, J. A. *Science* **1998**, *280*, 425.

(4) Davies, J. H. *The Physics of Low-Dimensional Semiconductors*; Cambridge University Press: Cambridge, 1998; Chapter 4.

(5) Switzer, J. A.; Shane, M. J.; Phillips, R. J. *Science* **1990**, *247*, 444.

(6) Switzer, J. A.; Raffaele, R. P.; Phillips, R. J.; Hung, C.-J.; Golden, T. D. *Science* **1992**, *258*, 1918.

(7) Switzer, J. A.; Hung, C.-J.; Breyfogle, B. E.; Shumsky, M. G.; Van Leeuwen, R.; Golden, T. D. *Science* **1994**, *264*, 1573.

(8) Phillips, R. J.; Golden, T. D.; Shumsky, M. G.; Bohannan, E. W.; Switzer, J. A. *Chem. Mater.* **1997**, *9*, 1670.

(9) Shima, M.; Salamanca-Riba, L.; Moffat, T. P.; McMichael, R. D.; Swartzneruber, L. J. *J. Appl. Phys.* **1998**, *84*, 1504.

(10) Switzer, J. A.; Hung, C.-J.; Huang, L.-Y.; Switzer, E. R.; Kammler, D. R.; Golden, T. D.; Bohannan, E. W. *J. Am. Chem. Soc.* **1998**, *120*, 3530.

(11) Switzer, J. A.; Maune, B. M.; Raub, E. R.; Bohannan, E. W. *J. Phys. Chem. B* **1999**, *103*, 395.

(12) Lincot, D.; Kampmann, B.; Mokili, B.; Vedel, J.; Cortes, R.; Froment, M. *Appl. Phys. Lett.* **1995**, *67*, 2355.

(13) Pauporte, T.; Lincot, D. *Appl. Phys. Lett.* **1999**, *75*, 3817.

(14) Switzer, J. A.; Shumsky, M. G.; Bohannan, E. W. *Science* **1999**, *284*, 293.

(15) Bohannan, E. W.; Shumsky, M. G.; Switzer, J. A. *Chem. Mater.* **1999**, *11*, 2289.

(16) Vertegel, A. A.; Shumsky, M. G.; Switzer, J. A. *Angew. Chem., Intl. Ed.* **1999**, *38*, 3169.

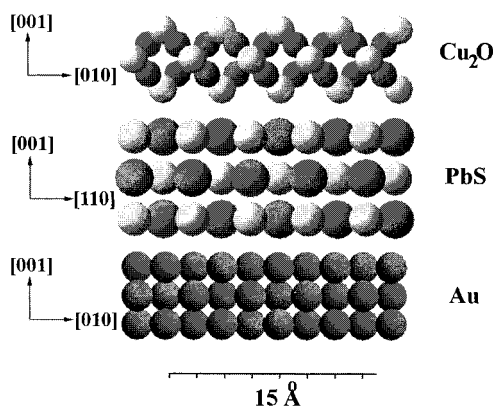


**Figure 1.** Schematic of the  $\text{Cu}_2\text{O}/\text{PbS}/\text{Au}$  (100) epitaxial heterojunction. Only one-unit-cell-thick layers are shown for  $\text{PbS}$  and  $\text{Cu}_2\text{O}$ , although the real thickness of the films is about  $0.5\ \mu\text{m}$ . The actual thickness of the Au substrate is 1 mm. The metal atoms are dark, and the nonmetals atoms are light. The arrows to the left of each structure show the crystallographic directions for each layer.

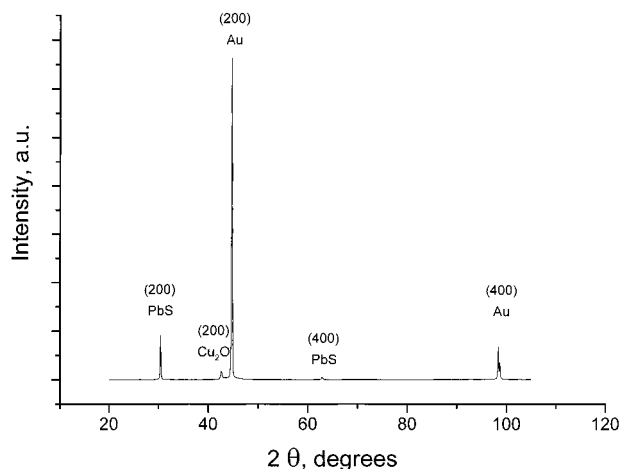


**Figure 2.** X-ray diffraction pattern probing the out-of-plane orientation of a heterostructure consisting of  $0.5\text{-}\mu\text{m}$ -thick  $\text{PbS}$  and  $\text{Cu}_2\text{O}$  films sequentially electrodeposited onto single-crystal Au(100). Rocking curves for the (200) reflections of Au,  $\text{PbS}$ , and  $\text{Cu}_2\text{O}$  have fwhm of  $0.6^\circ$ ,  $1.1^\circ$ , and  $2.3^\circ$ , respectively.

The large mismatch in the  $\text{Bi}_2\text{O}_3/\text{Au}$  (35.3%) and  $\text{PbS}/\text{Au}$  (45.5%) epitaxial systems was accommodated by the formation of coincidence lattices, in which the film was rotated relative to the Au substrate. The mismatch in the  $\text{Cu}_2\text{O}/\text{Au}$  system was only 4.4%, and no rotation of the film was observed. In the present paper we report the epitaxial electrodeposition of a  $\text{Cu}_2\text{O}/\text{PbS}$  heterojunction on single-crystal Au(100) (see Figure 1).

Both  $\text{PbS}$  and  $\text{Cu}_2\text{O}$  are p-type semiconductors.  $\text{PbS}$  is a low band-gap (0.4 eV) semiconductor with a face centered cubic (fcc) structure (space group  $Fm\bar{3}m$  and lattice parameter  $a = 0.5933\ \text{nm}$ ).  $\text{Cu}_2\text{O}$  has a larger band gap of 2.0 eV and adopts a primitive cubic structure ( $Pn\bar{3}m$ ,  $a = 0.4270\ \text{nm}$ ). The structure of Au is face centered cubic ( $Fm\bar{3}m$ ,  $a = 0.4079\ \text{nm}$ ).

The first step for the preparation of the  $\text{PbS}/\text{Cu}_2\text{O}$  heterojunction was the electrodeposition of an epitaxial  $\text{PbS}$  film of about  $0.5\ \mu\text{m}$  thickness onto a Au(100) substrate. The deposition was carried out as described

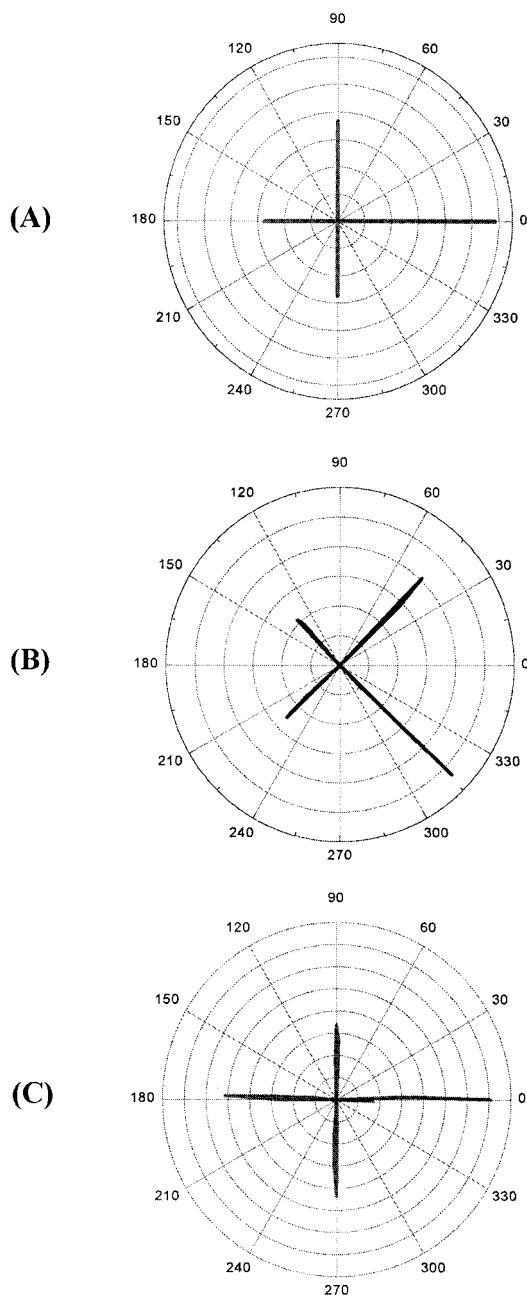


**Figure 3.** Azimuthal scans for (A) the (220) reflection of Au ( $2\theta = 64.58^\circ$ ), (B) the (220) reflection of PbS ( $2\theta = 43.05^\circ$ ), and (C) the (110) reflection of  $\text{Cu}_2\text{O}$  ( $2\theta = 29.55^\circ$ ). Each scan was acquired for the sample tilted  $45^\circ$  with respect to the plane of the goniometer. The (220) reflections for PbS are rotated  $45^\circ$  with respect to those of Au and  $\text{Cu}_2\text{O}$ . The average fwhm for the peaks are  $0.5^\circ$ ,  $1.6^\circ$ , and  $2.8^\circ$  for Au, PbS, and  $\text{Cu}_2\text{O}$ , respectively.

elsewhere.<sup>16</sup> The sample was then rinsed with HPLC-grade water, dried, and immersed in the second deposition solution, which contained copper(II) lactate at pH = 9.0. The electrodeposition of the  $0.5\text{-}\mu\text{m}$ -thick  $\text{Cu}_2\text{O}$  film was performed as described earlier.<sup>15</sup> Both films were deposited galvanostatically using current densities of 0.1 and 0.05  $\text{mA}/\text{cm}^2$  for the PbS and  $\text{Cu}_2\text{O}$  films, respectively.

X-ray diffraction (XRD) experiments were performed with a Scintag XDS-2000 diffractometer using  $\text{Cu K}\alpha$  radiation. Figure 2 shows the XRD pattern of the sample. Only the (200) and (400) reflections are ob-

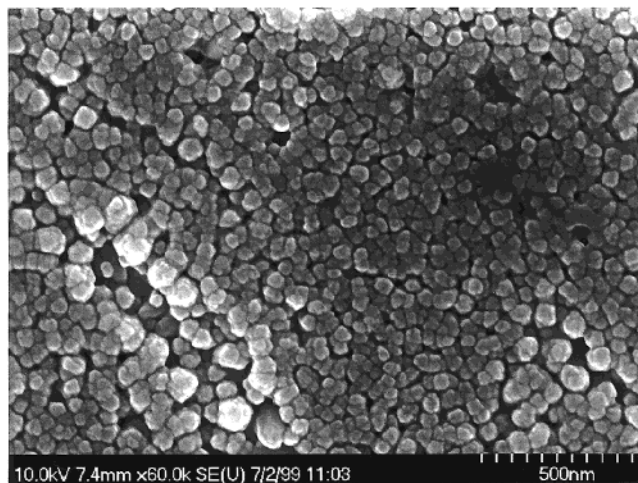


**Figure 4.** SEM micrograph of the  $\text{Cu}_2\text{O}$  overlayer. The SEM measurement was performed ex situ on an Hitachi model S4700 cold field emission scanning electron microscope.

served for both deposited films, indicating an out-of-plane orientation. Because of the higher value of the atomic scattering factor for Pb atoms, the relative intensities of the (200) peaks for PbS and  $\text{Cu}_2\text{O}$  are significantly different although both films have the same nominal thickness.

Figure 3 shows the (220) azimuthal scans for Au and PbS and the (110) azimuthal scan for  $\text{Cu}_2\text{O}$ . The (110) reflection is symmetry-forbidden for Au (fcc structure), but allowed for  $\text{Cu}_2\text{O}$  (primitive cubic structure). Therefore, by choosing the (110) reflection of  $\text{Cu}_2\text{O}$  we avoid possible overlapping of the Au and  $\text{Cu}_2\text{O}$  peaks, so that the reflections observed in the azimuthal scan correspond to the film only. The expected 4-fold symmetry is observed in all three azimuthal scans in Figure 3. However, the (220) reflections of PbS appear at azimuthal angles rotated  $45^\circ$  with respect to the reflections of Au and  $\text{Cu}_2\text{O}$ . This means that although the PbS layer adopts the same (100) out-of-plane orientation as the substrate, the PbS structure is rotated  $45^\circ$  in plane with respect to the Au. An interface model consistent with this rotation is  $\text{Au (100)} / (\sqrt{2} \times \sqrt{2} R 45^\circ) - \text{PbS (100)}$ . Formation of this coincidence lattice decreases the large lattice mismatch between PbS and Au (45.5%) to +2.9%. The lattice mismatch between the second and the third layers is -38.9%. To accommodate this large mismatch, the cuprous oxide layer rotates  $45^\circ$  more in the plane of the substrate. The interface model of this junction is  $\text{PbS (100)} / (\sqrt{2} \times \sqrt{2} R 45^\circ) - \text{Cu}_2\text{O (100)}$ , and the lattice mismatch is +1.8%. Thus, all crystallographic directions of the  $\text{Cu}_2\text{O}$  film coincide with those of the substrate, as we observed previously in the case of electrodeposition of individual  $\text{Cu}_2\text{O}$  films on the Au(100) single crystal.<sup>15</sup>

An SEM micrograph of the  $\text{Cu}_2\text{O}$  layer is shown in Figure 4. The SEM view of the lead sulfide underlayer is similar to that presented in ref 16 and contains smooth rectangular features. The cuprous oxide film consists of unfaceted grains with the size of about 50 nm. Since the film thickness is  $\sim 10$  times larger than the average grain size, we suppose that the  $\text{Cu}_2\text{O}$  film has a columnar structure with each individual column growing epitaxially on top of PbS. Cross-sectional electron microscopy of these materials is in progress to

verify this columnar structure and to determine the abruptness of the Cu<sub>2</sub>O/PbS interface.

The particulate structure of the Cu<sub>2</sub>O layer in the heterojunction is not ideal for the production of layered nanostructures, but it may be desirable for dye-sensitized photoelectrochemical cells, since the semiconductor–solution interfacial area should be large. Grätzel and co-workers have produced efficient photoelectrochemical cells based on dye-sensitized nanoporous TiO<sub>2</sub>,<sup>17</sup> and Hara and co-workers have reported the photosplitting of water on nanocrystalline Cu<sub>2</sub>O.<sup>18</sup> The

Cu<sub>2</sub>O in the present work should have the high surface area of a particulate semiconductor, but the epitaxial nature of the layer should provide more effective charge transport for the photogenerated carriers.

**Acknowledgment.** This work was supported by National Science Foundation grants CHE-9816484 and DMR-9704288, and the University of Missouri Research Board.

CM9907054

---

(17) O'Regan, B.; Grätzel, M. *Nature* **1991**, 353, 737.

(18) Hara, M.; Kondo, T.; Komoda, M.; Ikeda, S.; Shinohara, K.; Tanaka, A.; Kondo, J.; Domen, K. *Chem. Commun.* **1998**, 357.